Geochemistry, Geophysics, Geosystems®

AGU ADVANCING EARTH AND SPACE SCIENCE

RESEARCH ARTICLE
10.1029/2021GC009903

Key Points:

- The climate over mid-latitude Asia presented seasonal response to abrupt climate events during the last glacial
- Spring climate is more sensitive to millennial-scale abrupt events than summer
- The weakening and closing of the Atlantic meridional overturning circulation influence the seasonal response

Correspondence to:
J. Jia and D. S. Xia,
jiaj@zjnu.edu.cn;
dsxia@lzu.edu.cn

Citation:
Fan, Y., Jia, J., Xia, D., Meadows, M., & Wang, Z. (2021). Seasonality of response to millennial-scale climate events of the last glacial: Evidence from loess records over mid-latitude Asia. *Geochemistry, Geophysics, Geosystems*, *22*, e2021GC009903. https://doi.org/10.1029/2021GC009903

Received 11 MAY 2021
Accepted 4 OCT 2021

Seasonality of Response to Millennial-Scale Climate Events of the Last Glacial: Evidence From Loess Records Over Mid-Latitude Asia

Yijiao Fan[1,2], Jia Jia[2], Dunsheng Xia[1], Michael Meadows[2,3,4], and Zhiyuan Wang[2]

[1]Key Laboratory of Western China's Environmental System (Ministry of Education), College of Earth and Environmental Sciences, Lanzhou University, Lanzhou, China, [2]College of Geography and Environmental Sciences, Zhejiang Normal University, Jinhua, China, [3]Department of Environmental & Geographical Science, University of Cape Town, Rondebosch, South Africa, [4]School of Geography and Ocean Sciences, Nanjing University, Nanjing, China

Abstract Although difficult to resolve, seasonality is an important element in considering paleoenvironmental records and simulated results, and it is therefore critical to address this shortcoming in order to develop more accurate reconstructions of past climate. In this study, climatic proxies with seasonal implications (magnetic susceptibility and mean grain size) are analyzed for several high-resolution loess sections from mid-latitude Asia using the Ensemble Empirical Mode Decomposition (EEMD) to detect their response to millennial-scale oscillations during the last glaciation. In so doing, we are capable to estimate the amplitude and relative contribution of the reconstructed climate components. Combined with an analysis of modern processes, magnetic susceptibility (χ) can be interpreted as representing summer and spring precipitation, while mean grain size (Mz) can be interpreted as representing spring and summer dust activity in the Chinese Loess Plateau (CLP) and southern central Asia (SCA), respectively. Our results show that the spring and summer signals are clearly correlated with Heinrich events, but that the spring signal is more prominent than the summer signal during Dansgaard-Oeschger (D-O) oscillations of the last glacial. These results are consistent with modeled simulations. It is proposed that weakening or complete shutdown of AMOC influences the response of seasonal signals to abrupt climate events. The study highlights the need for further high-resolution climate proxies with robust seasonality indicators in order to develop a deeper understanding of the response of mid-latitude Asia to rapid climate events.

1. Introduction

In the context of anthropogenic climate change, the need for an accurate, detailed understanding of the earth system has become increasingly important. Geological records provide climatic boundary conditions that are pivotal in numeric reconstructions of past climates. More importantly, proxy climatic records reveal the sensitivity of climate processes at decadal to millennial timescales and unforeseen non-linear responses. Paleoclimatic reconstructions are generally based on so-called proxies and numerical simulations, or their combinations thereof (e.g., Chen et al., 2016; Kang et al., 2020; Li et al., 2020). Paleoclimatic proxies yield indirect signals of climatic characteristics, according to the means by which the proxies themselves respond to changes in the environment. Climatic simulations deliver approximate representations of paleoclimate change which can be deployed to predict future climate under different boundary conditions. Nevertheless, paleoclimate reconstructions based on geological records may sometimes differ from—or even contrast sharply with simulations (e.g., Brewer et al., 2007; Jiang et al., 2012; Liu, Zhu, et al., 2014; Lohmann et al., 2013; Lu et al., 2018; Schneider et al., 2010; Sundqvist et al., 2010) and critical reexamination of the proxy and modeled results may be necessary (Liu, Zhu, et al., 2014; Lohmann et al., 2013). In some cases, the errors lie with the climate models owing to their limited temporal resolution or due to climate sensitivity biases that arise in the simulation process (Jin et al., 2007; Liu, Zhu, et al., 2014). In still other cases, climate proxies are challenging to interpret due to, for example inherent uncertainties associated with biological processes, which are themselves dependent on climate factors and may be sensitive to seasonal differences. Identifying seasonal responses and sensitivity to climate parameters are important considerations in constructing paleoclimates (Bova et al., 2021; Liu, Zhu, et al., 2014), although they are usually highly complex and difficult to resolve.

During the last glaciation, rapid fluctuations of the climate system have been described from the northern high latitudes and recorded in high-resolution archives such as ice cores from Greenland and ice-rafted deposits in the Atlantic Ocean (Bond et al., 1993; Dansgaard et al., 1993; Grootes et al., 1993). These signals of millennial-scale climate oscillations have now been found in a diverse range of geological archives, including, *inter alia*, deep sea sediments (Altabet et al., 2002; Dannenmann et al., 2003; Zhao et al., 2006), cave stalagmites (Burns et al., 2003; Cheng et al., 2006; Wang et al., 2008), loess deposits (Ding et al., 1998; Porter & An, 1995; Yang & Ding, 2014). Simulation studies have suggested that such millennial-scale climatic signals can be widespread and affect distant regions such as continental Asia, the Pacific Ocean and Antarctica through atmospheric and oceanic circulation (Clement & Peterson, 2008; Jin et al., 2007; Sun et al., 2012; Wu et al., 2008; Zhang & Delworth, 2005). However, the response of different regions and various geological deposits to these rapid climatic events may be inconsistent (e.g., Ahn & Brook, 2008; Blunier & Brook, 2001; Cheng et al., 2020; Clement & Peterson, 2008), in part due to processes associated with the bipolar seesaw, as well as variations in the sensitivity of the deposits themselves.

Long, continuous loess sequences accumulated over an extended timescale are widely distributed in mid-latitude Asia (e.g., Ding et al., 2002; Porter, 2001) and provide valuable information and insight in understanding environmental evolution, especially during the Quaternary. Loess-paleosol sequences in the CLP have revealed dynamics of the east Asian Monsoon (EAM) at the orbital, suborbital and millennial scales (Ding et al., 1995; Li et al., 2015; Sun & Guo, 2017). Numerous studies have reported rapid changes in the EAM since MIS 7 that can be compared with, for example, high resolution stalagmite and Greenland ice core records (Guo et al., 2020; Sun et al., 2012, 2016; Wang et al., 2020; Yang & Ding, 2014). However, while EAM fluctuations are well represented in the CLP records, moisture variations here appear to be less sensitive to abrupt climate events compared with the situation further west where moisture changes during warm interstadials have been adequately reconstructed (Jia et al., 2019; Wang et al., 2018). Variations in loess particle size, associated with wind intensity in central and east Asia, reveal substantial fluctuations during the last glaciation that appear to be well correlated with abrupt climate changes in the northern high-latitudes (An et al., 1991; Li et al., 2016, 2018; Song et al., 2018; Sun et al., 2012; Vandenberghe et al., 2006; Yang & Ding, 2014; Zhang et al., 2015). Different climate proxies seem to present distinct signatures of these abrupt climate events, which may be attributed to seasonal biases in response to climate change. For example, given that the timing of precipitation and wind intensity differs markedly between the CLP and SCA, comparing geological records between these regions may facilitate a more nuanced understanding of seasonality changes during rapid climate events of the last glacial. Here, we present evidence from high-resolution loess sections located in the CLP and SCA, which combined with interpreted proxies, are used to detect seasonal changes in the response to abrupt climate events of the last glacial. In so doing, we develop an improved understanding of the different responses in geological deposits over mid-latitude Asia to high latitude climate events.

2. Materials and Methods

2.1. Physical Environmental Setting

The CLP is situated in the eastern part of mid-latitude Asia and south of the arid-semiarid desert regions in northern China (Figure 1). The region is characterized by quasi-continuous loess-paleosol sequences that provide a rich, well-preserved paleoclimatic archive (Liu, 1985). Due to the thermal capacity difference of the Asian continent and western Pacific Ocean, the climate of the CLP is dominated by EAM circulation which carries warm, moisture-bearing air masses from the Pacific Ocean in the summer, and cold and dry air masses from the northern high-latitudes in winter. Mean annual precipitation and temperature decreases from the southeast to the northwest across the CLP with corresponding vegetation changes from forest to steppe and desert steppe (Yu et al., 2000).

SCA is situated to the southern part of arid central Asia and, due to its great distance from the ocean, is characterized by a continental arid climate (Schiemann et al., 2008). From the Caspian Sea in the west to the western Pamir Mountains, the region is occupied by extensive areas of loess, desert, and high mountains (Ding et al., 2002). The region is influenced strongly by the Westerlies, which contribute most of the annual precipitation in winter and spring when humid air masses are transported from the Mediterranean, Black and Caspian Seas (Jin et al., 2012), while in summer, the subtropical high pressure is dominant (Karger

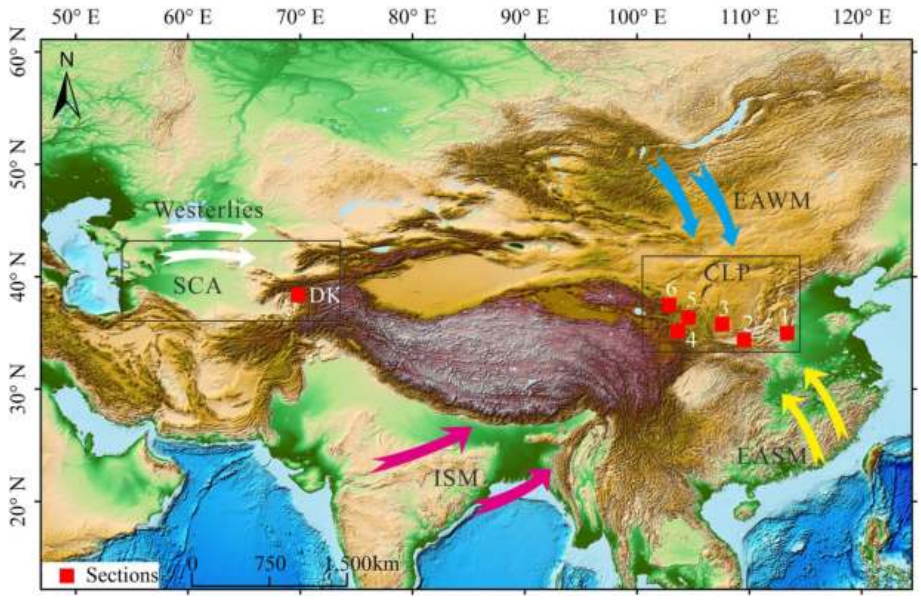

Figure 1. The loess sections in the Chinese Loess Plateau (CLP) and southern central Asia (SCA) and modern atmospheric circulation patterns that include the east Asia summer monsoon (EASM, yellow arrow), east Asia winter monsoon (EAWM, blue arrow), Indian summer monsoon (ISM, pink arrow), and Westerlies (white arrow). Loess sections (1–6) on the CLP are MS (Wang et al., 2020), WN (Sun et al., 2010), XF (Sun et al., 2010), YB (Rao et al., 2013), JY (Sun et al., 2010), GL (Sun et al., 2016), respectively. DK section (Jia et al., 2018) locates in the eastern part of SCA.

et al., 2016). Vegetation of this region varies from desert to grassland depending on the mean annual precipitation and altitude.

2.2. Data Sources and Processing

Six continuous loess sections located in the CLP (MS, WN, XF, YB, JY, and GL) and one in SCA (DK) (Figure 1 and Table 1) were selected based on two criteria, *viz* continuous sediment accumulation from the last glaciation or earlier, and the availability of published data on the parameters χ and Mz. We focus on the period between 65 and 25 ka because the millennial-scale climate oscillations have been shown to be relatively distinct and continuous during that time (Sun et al., 2010; Wang et al., 2018). The NGRIP $\delta^{18}O$ record (North Greenland Ice Core Project Members, 2004) was also used for comparison in order to reveal possible teleconnections with high latitude climate events.

Ensemble Empirical Mode Decomposition (EEMD) (Huang et al., 1998) was applied to linearly interpolated χ and Mz data at 100-year intervals in order to quantify their response to millennial-scale climate oscillations. The EEMD method is based on noise-assisted data analysis, which takes the average value of multiple measurements and obtains the ensemble means of corresponding intrinsic mode functions (IMFs) as the final outcomes (Huang & Wu, 2008; Huang et al., 1998; Wu & Huang, 2009). The EEMD method has been successfully applied to decipher multiscale variations in loess (Li et al., 2015; Wang et al., 2020), speleothem (Cai et al., 2015; Tan et al., 2020) and tree-ring records (Liu et al., 2017). A detailed explanation of the process is available in the EEMD code program instructions (Wu & Huang, 2009). In addition, REDFIT software was used to obtain spectral frequencies of the different loess proxies and NGRIP $\delta^{18}O$ data (Schulz & Mudelsee, 2002).

Modern values for seasonal variations in precipitation, soil moisture, surface wind speed and normalized differential vegetation index (NDVI) values were used in order to establish climate indicators for the proxies. Climate reanalysis data for monthly precipitation, soil moisture and surface wind speed covering the period 1982–2006 were obtained for both the CLP and SCA from the National Center for Environmental Prediction/National Center for Atmospheric Research (NCEP/NCAR) (http://www.esrl.noaa.gov/psd/data/gridded/, Kalnay et al., 1996). NDVI values for the same period are available at https://climatedat-

Table 1
Data Sources of the Sections Used in This Study

Section	Location	Proxies	Sampling interval (cm)	Thickness (25–65 ka) (m)	Chronology framework	Sedimentation rate (cm/kyr)	Reference
CLP							
MS	34°57′28.3″ 113°22′13.7″	χ, Mz	5	~38	OSL and tie points with speleothem $\delta^{18}O$	~61.57	Qiu and Zhou (2015) and Wang et al. (2020)
WN	34°21′ 109°31′	χ, Mz	5	~8.5	Tie points with JY	~12.42	Sun et al. (2010)
XF	35°47′ 107°36′	χ, Mz	5	~10	Tie points with JY	~15.38	Sun et al. (2010)
YB	35°9′ 103°37′48″	χ, Mz	4	~24.5	OSL	~42.84	Lai and Wintle (2006), Lai et al. (2007), and Rao et al. (2013)
JY	36°21′ 104°37′	χ, Mz	2	~25	OSL	~48.34	Sun et al. (2010)
GL	37°29′ 102°52′	χ, Mz	2	~19	OSL	~38.54	Sun et al. (2016)
SCA							
DK	38°23′44″ 69°50′1″	χ, Mz	2	~17.5	Tie points with NGRIP $\delta^{18}O$	~42.70	Wang et al. (2018) and Lu et al. (2020)

aguide.ucar.edu/climate-data/ndvi-normalized-difference-vegetation-index-noaa-avhrr. Even though the impact of human activity on the surface vegetation cannot be eliminated in the CLP, especially given the dominant type of vegetation, we focus only on the influence of seasonal variations on vegetation growth, rather than changes in species, distribution, etc. Accordingly, remote mountainous areas likely to have been less affected by human activity were selected to observe the natural seasonal variation of vegetation when selecting the NDVI data.

3. Interpretation of Climate Proxies

3.1. Magnetic Susceptibility (χ)

Magnetic susceptibility records in loess sequences have been used successfully to indicate regional precipitation in the CLP and SCA (e.g., Tajikistan) (An et al., 1991; Ding et al., 2002; Dodonov et al., 2006; Wang et al., 2018; Yang et al., 2006). Higher χ values are mainly related to the mass of ultra-fine magnetite and/or maghemite generated during the pedogenesis that in turn correlates with precipitation and biogeochemical activity (Forster & Heller, 1997; Jia et al., 2018; Maher, 1998; Torrent et al., 2006). Although it is widely recorded that soil development and biogeochemical processes in soils are related to seasonal changes (Deng et al., 2007; Meng et al., 1997), little attention has been paid to using the paleosol record to reconstruct variations in seasonality. In fact, soil moisture content and its seasonal variation are considered essential factors for the formation of fine-grained ferrimagnetics (Maher, 1998). In addition, analysis of the magnetic characteristics of modern loessic soils and loessic paleosols shows that newly formed magnetite/maghemite with strongly magnetic fine particles is formed mainly in the wet season, rather than throughout the year (Yang & Jia, 2021), thus confirming the differential seasonal development of pedogenesis under different climatic conditions (Balsam et al., 2011).

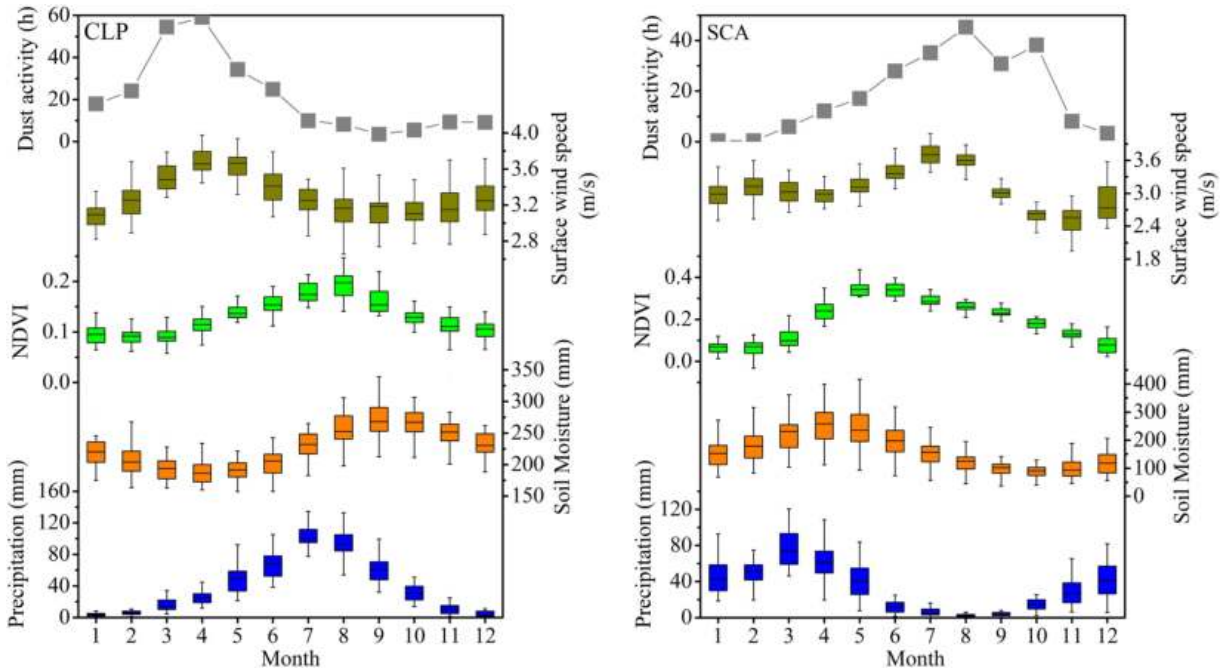

Figure 2. Monthly comparisons between precipitation, soil moisture, normalized differential vegetation index and surface wind speed (1982–2006) over the Chinese Loess Plateau and southern central Asia. Data on dust activity are modified after Finaev (2014) and Ning et al. (2005).

On the base of modern observations, both soil moisture and vegetation growth, here indicated by NDVI, vary seasonally with precipitation (Figure 2) and exhibit higher values during summer in the CLP, and spring in SCA. The relatively high NDVI values in summer months (June–September) in SCA may indicates that the vegetation growth exhibits a non-linear response to the precipitation, because the temperature also has effect on vegetation growth. As to clarify the effect of seasonal precipitation on the vegetation growth in SCA, Pearson correlation coefficients between precipitation and NDVI monthly values from 1982 to 2006 demonstrate that the moisture required to promote vegetation growth is mainly supplied by precipitation in the spring months (Figure 3). Generally, precipitation augments soil moisture and promotes vegetation growth, which enhances pedogenesis and, in turn, results in higher soil χ values. Central Asia was characterized by a winter-spring rainfall maximum for at least past 1.77 Myr (Yang & Ding, 2006), and east Asia was characterized a typical monsoon climate with dominant summer precipitation during the Quaternary (Wang, 2009). In two regions (CLP and SCA) with similar annual mean temperature, magnetic particles formed in soils developed in areas dominated by winter-rain area are finer than those found in summer-rain areas (Yang & Jia, 2021). Since the individual size of crystal particles is related to the temperature, it can be assumed that the magnetic susceptibility of soils in winter-rain areas record mainly the climate signal in spring, while those in the summer-rain areas record mainly the climate in summer (Yang & Jia, 2021).

3.2. Mean Grain Size (Mz)

Variations of Mz in loess reflect wind energy and this relationship has been applied in many paleoclimate reconstructions (Li et al., 2015; Sun et al., 2012, 2015). In general, Mz exhibits glacial-interglacial, stadial-interstadials and millennial-scale fluctuations, with relatively coarser values in glacial and stadial periods, during which the dust accumulation rate and dust flux are greater (Sun et al., 2021). Variations of Mz can be affected by wind strength, source-to-sink distance and expanding desert margin (Ding et al., 1999; Yang & Ding, 2008). It has been noted that loess in the CLP is comprises mainly dust from the Gobi and deserts of northern China (Sun, 2020; Sun et al., 2001). Under the condition of constant dust source, the influence of source-to-sink distance is mainly reflected in the spatial variation of loess Mz, as the greater the distance from source, the finer the loess Mz (Sun et al., 2021). The influence of desert expansion on the loess Mz values between 65 and 25 ka is likely to be only minor, since, between the Last Glacial Maximum and

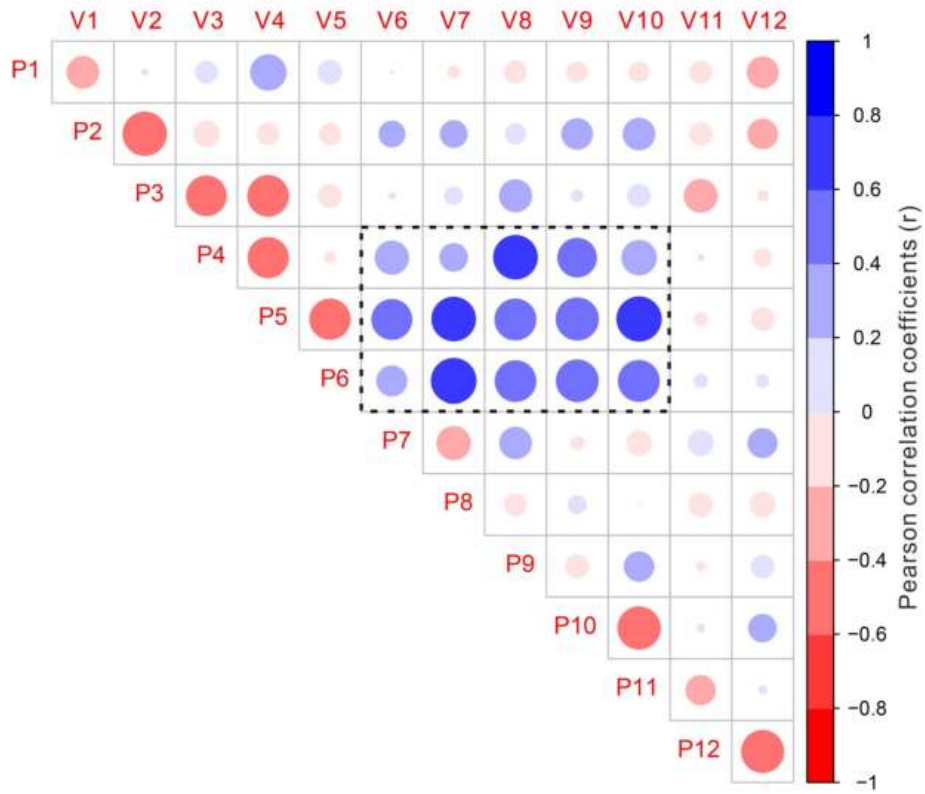

Figure 3. Pearson correlation coefficients (*r*) between precipitation and normalized differential vegetation index (NDVI) monthly values over southern central Asia. V1–V12 and P1–P12 represent NDVI and precipitation from January to December, respectively.

Holocene Optimum, deserts in northern China extended only 20 km southwards (Lu et al., 2013). In the DK section, coarser Mz signal is accompanied by increased humidity during interstadial periods of the last glacial (Figure 4g) and coarser Mz is unlikely to be induced by desert expansion. Therefore, the variation of loess Mz between 65 and 25 ka is affected mainly by wind strength, with higher values indicating stronger winds, typically accompanied by surface dust activity and transporting coarser particle size fraction to dust accumulation areas (An et al., 1991; Xiao et al., 1995). Dust activity is in general associated with higher surface wind speeds that promote greater dust flux and coarser particle size (Finaev, 2014; Li, Song, Kaskaoutis, et al., 2019; Sun et al., 2001). In line with observations, longer periods (1982–2006) of dust activity usually occur in seasons with higher surface wind speeds, lower precipitation, soil moisture and vegetation cover, exhibiting higher values during spring in the CLP and summer in SCA, respectively (Figure 2). There are seasonal differences in precipitation both in the CLP and central Asia during the last glacial as discussed above, so the dust activity would also be seasonal difference. During the last glaciation, variation of the Westerlies and EAM parallels that of the Greenland temperature and the Atlantic meridional overturning circulation at the millennial timescale (Li, Song, Yin, et al., 2019; Sun et al., 2012), which indicated that the surface dust activity and dust flux are not constant throughout the year, rather than exhibited seasonal variations.

From the modern analysis, the precipitation, soil moisture and NDVI that promote the pedogenesis and the surface dust activity do show seasonal variations (Figure 2). Even though the loess surface may be disturbed by other factors after pedogenesis and dust activity, the pedogenesis mainly occurs in the season with more precipitation and the dust activity occurs in the season with higher surface wind speed. Affected by the sedimentation rate, sample size and type, aeolian loess deposition cannot directly record seasonal climate changes like a varved lake, but its climatic proxy can at least reflect the average seasonal conditions in several decades. On the basis of modern processes, it is therefore proposed that χ values of loess can be used as a proxy for summer precipitation in the CLP and spring precipitation in SCA, and that the Mz can

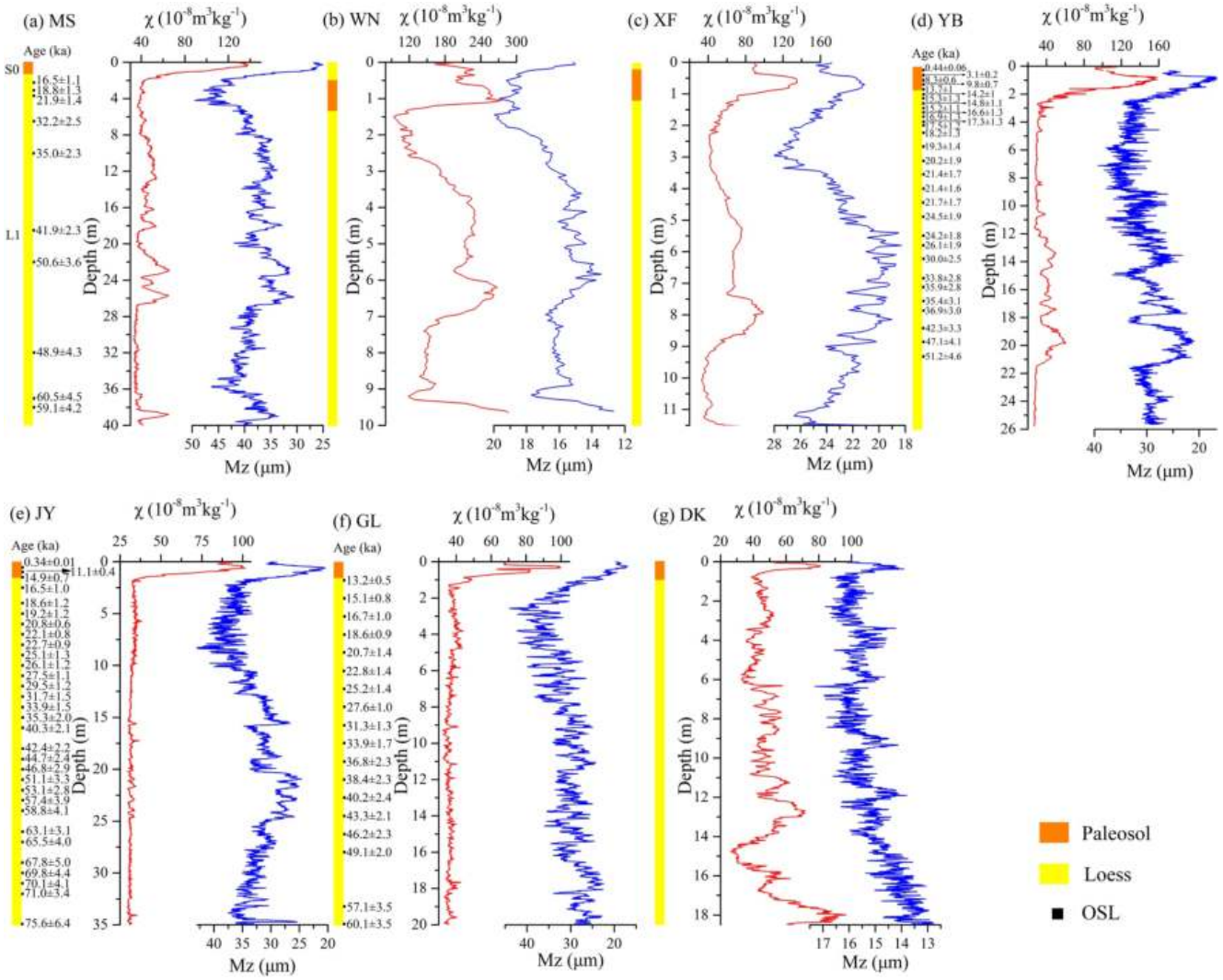

Figure 4. Stratigraphy, χ, Mz, and OSL ages for the seven loess sections in the Chinese Loess Plateau and southern central Asia.

be interpreted as indicative of spring dust activity in the CLP and summer dust activity in SCA at millennial scale during the last glaciation.

4. Results

As shown in Figure 4, the amplitude of Mz variations in all sections is greater than that for χ, and the amplitude of χ variation is greater for the DK section than those in the CLP. In addition, WN and XF sections, located in the southern and central CLP, exhibit only minor millennial-scale variations in χ and Mz, which may be due to the relatively low sedimentation rate and intense pedogenesis that may compound oscillations at these time scales (Sun et al., 2010). We therefore excluded the WN and XF sections from further consideration. In JY and GL sections, χ values exhibit only low variability, which suggests that these records provide only weak climate signals, although the Mz record is characterized by higher frequency and abrupt oscillations. Accordingly, the χ data for YB, MS, and DK sections and Mz data for YB, JY, MS, and DK sections are selected to conduct the EEMD and spectral analysis.

Patterns of variation in the selected loess χ, Mz, and NGRIP $\delta^{18}O$ time series are analyzed using the EEMD and presented in Figures 5 and 6. Seven IMF are generated from the data. In order to account for noise in the data, IMF1 periodicities of less than 1 kyr were excluded from further consideration. Dominant periodicities

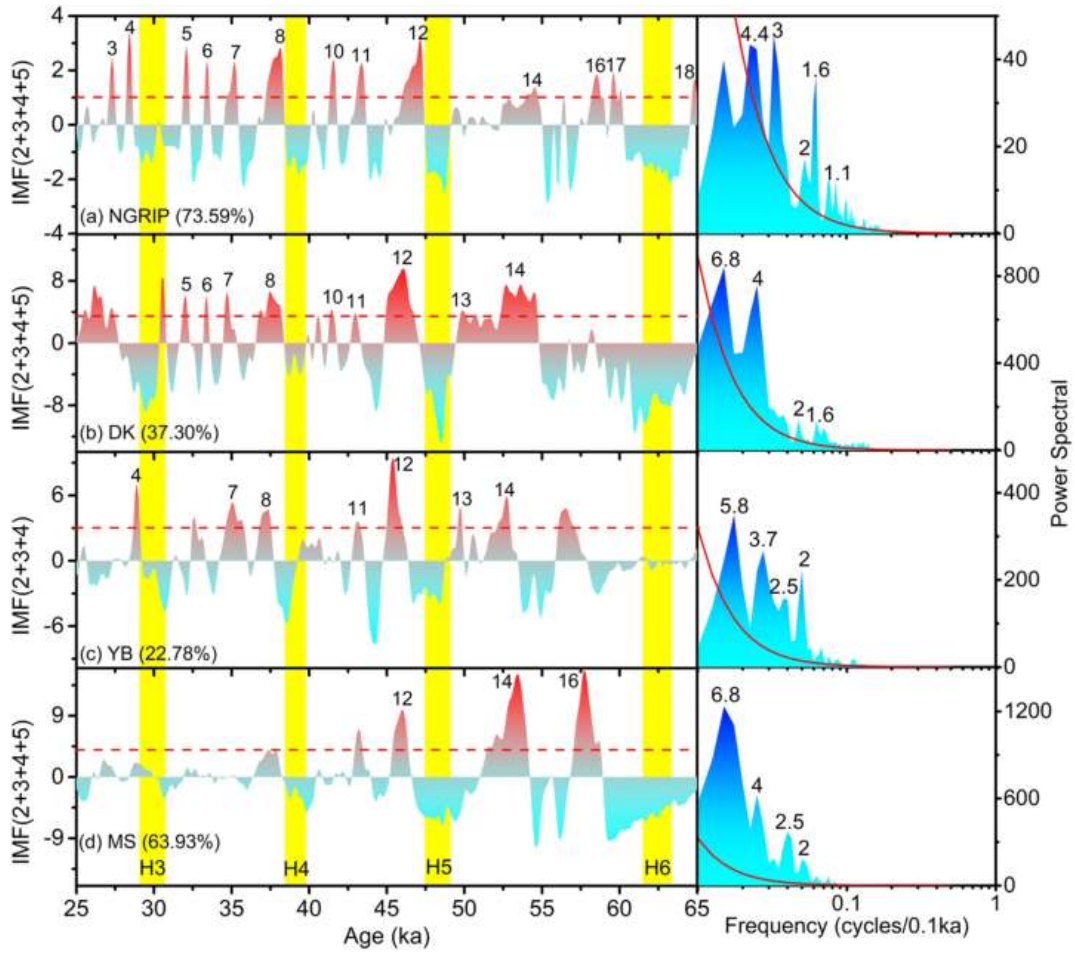

Figure 5. Comparisons of relative contributions of millennial-scale components (1–9 kyr) of χ in loess sections over the Chinese Loess Plateau and southern central Asia with the NGRIP ice-core $\delta^{18}O$ record (North Greenland Ice Core Project Members, 2004). Red dashed lines represent the threshold lines used for detecting abrupt climatic events. The yellow vertical bars indicate Heinrich events and black numbers indicate warm episodes. Results of spectral analysis of millennial-scale components are shown on the right with numbers indicating dominant periodicities and red lines represent the 95% confidence level.

of between 1 and 9 kyr are regarded as millennial-scale variations (Figures 5 and 6), while those greater than 9 kyr represent orbital scale variability (Figure 7). Relative contributions of the millennial-scale components of χ and Mz in the selected loess sections are 37.30% (DK), 22.78% (YB), 63.93% (MS) (Figure 5) and 69.26% (DK), 77.31% (YB), 38.67% (JY), 56.14% (MS) (Figure 6) respectively, compared to values in the NGRIP $\delta^{18}O$ record (73.59%). REDFIT spectral analysis was further carried out on the millennial-scale components with dominant periodicities as shown on the right of Figures 5 and 6. Two dominant rhythms are evident in the loess sequences, *viz.* ~8–4 and ~3.3–1 kyr, possibly corresponding to the Heinrich (~6 kyr) and Dansgaard-Oeschger (D-O) (~1.5 kyr) oscillations as recorded in the Greenland NGRIP $\delta^{18}O$ record and North Atlantic Ocean sediments (Bond et al., 1993; Dansgaard et al., 1993).

5. Discussion

5.1. Seasonal Variations in Response to Abrupt Climate Events

As shown in Figure 5, the existence of warming episodes and their relative amplitudes captured in the analyzed χ data for DK section are more prominent than those reflected in YB and MS sections. On the contrary, warming episodes captured in the analyzed Mz data for YB, JY, and MS sections in the CLP are more obviously than those indicated in the DK section, in which the oscillations above the red dotted line

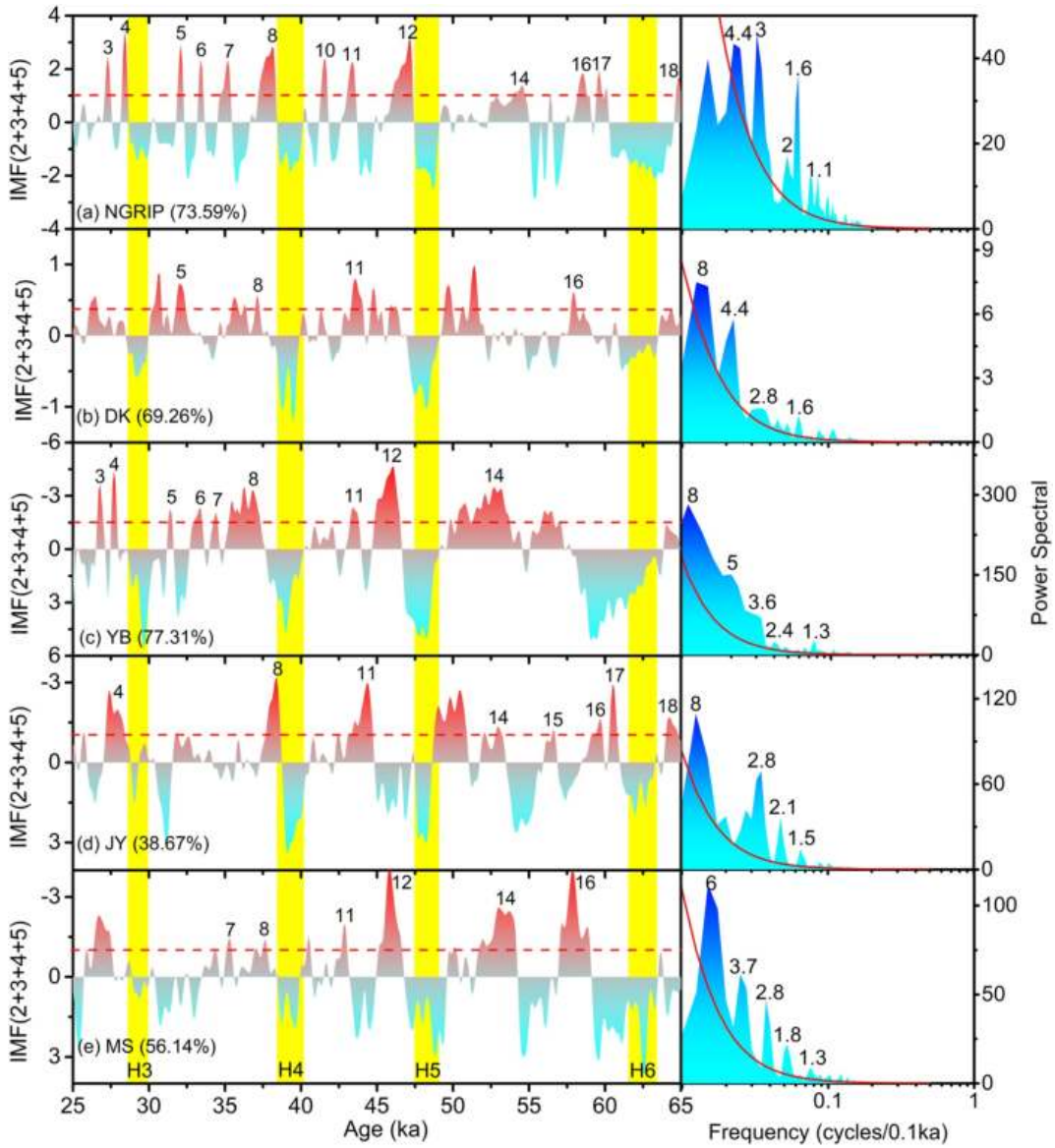

Figure 6. Comparisons of relative contributions of millennial-scale components (1–9 kyr) of Mz in loess sections over the Chinese Loess Plateau and southern central Asia with the NGRIP ice-core $\delta^{18}O$ record (North Greenland Ice Core Project Members, 2004). Other information is consistent with Figure 5.

do not appear to correspond clearly with variations in the NGRIP $\delta^{18}O$ record (Figure 6). Supported by our interpretation of χ and Mz as discussed above, the spring signals (precipitation in SCA and dust activity in the CLP) appears to be more responsive to abrupt climate events than summer signals (precipitation in the CLP and dust activity in SCA) during the D-O oscillations. As for Heinrich events, the seasonal signals in most sections exhibit large amplitude fluctuations in the analyzed values of χ and Mz, which is also evident in the spectral analysis that indicates 5.8–8 kyr periodicities (Figures 5b, 5c, 5f, and 6b–6f).

To verify the response of seasonal signals to rapid climatic events recorded in the studied proxies, we applied meltwater-forcing from the TraCE-21 ka transient simulation (Liu et al., 2009; Liu, Wen, et al., 2014) for the period since the last deglaciation during which the Heinrich 1 (H1), the Younger Dryas (YD), the Bølling-Allerød (B/A) events and the 8.2 ka event occurred. The simulation results (Figure 8) show that summer precipitation in the CLP and SCA is rather less sensitive to such forcing than spring precipitation, which fluctuates dramatically during the last deglaciation. During the Bølling and Allerød periods, sharply

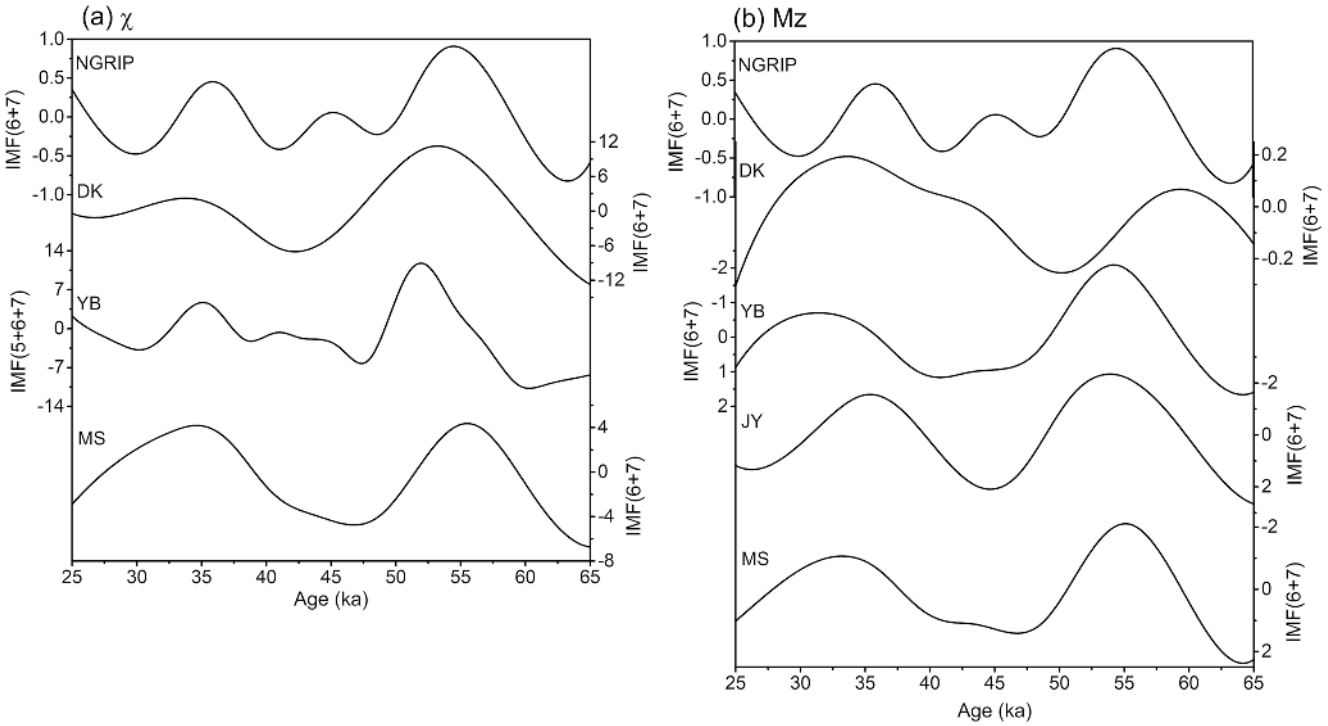

Figure 7. Orbital-scale components (>9 kyr) of χ and Mz in loess sections over the Chinese Loess Plateau and southern central Asia compared with the NGRIP ice-core $\delta^{18}O$ record (North Greenland Ice Core Project Members, 2004).

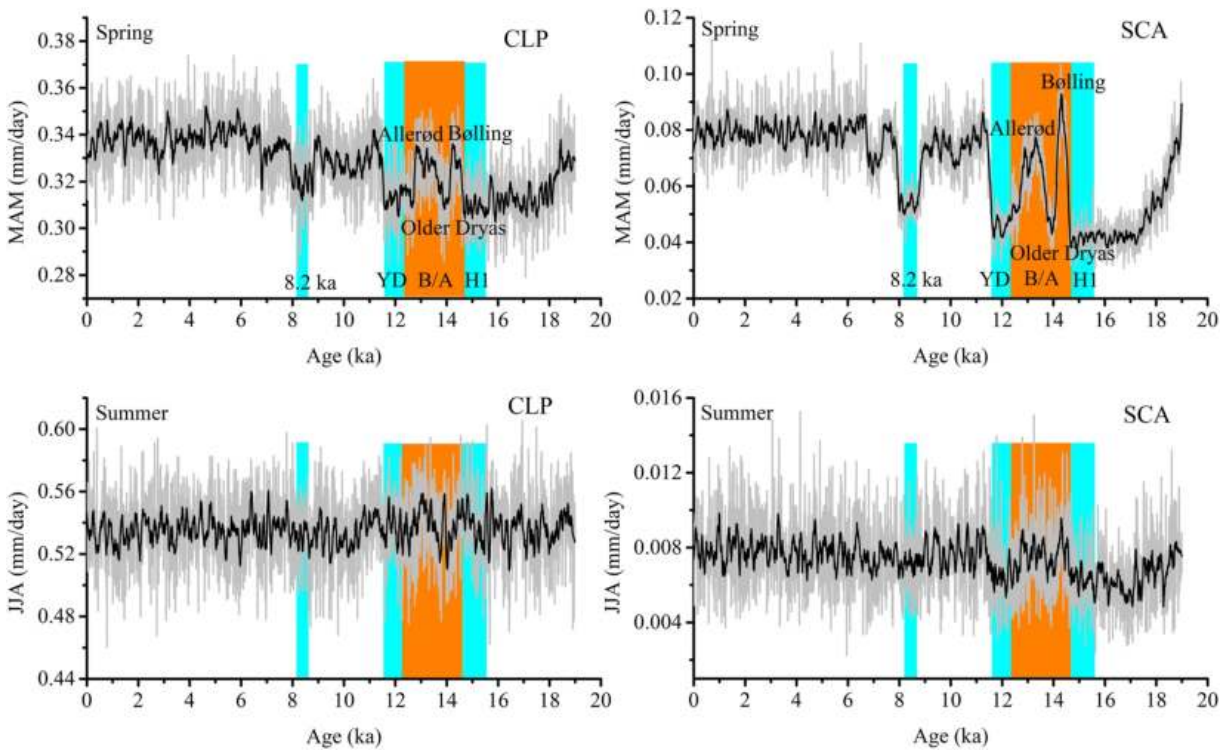

Figure 8. Simulated spring and summer precipitation variations since the last deglaciation over the Chinese Loess Plateau and southern central Asia. The black line represents smoothing values of the simulated spring and summer precipitation over this period.

decreasing spring precipitation is evident in the Older Dryas as observed in both the CLP and SCA. Moreover, abrupt cooling during the 8.2 ka event (Alley et al., 1997) and related fresh water injection (Barber et al., 1999; Kleiven et al., 2008) are also reflected in decreased spring precipitation over the CLP and SCA in the simulation results. In contrast, simulated summer precipitation appears to be less sensitive to meltwater forcing. In general, the simulated results support our interpretation of climatic proxies derived from the loess sections in demonstrating that, for mid-latitude Asia during the late Quaternary, proxy evidence for the spring months is more likely to reveal abrupt climatic events than evidence of changes in summer conditions.

5.2. Mechanisms Underlying Seasonal Differences

Various mechanisms have been proposed to explain the numerous abrupt climate events in the late Quaternary (Broecker, 1998; Clement & Peterson, 2008; Gildor & Tziperman, 2003; Knutti et al., 2004). Among these, thermohaline circulation - whereby Atlantic meridional overturning circulation (AMOC) weakens or shuts down when freshwater is discharged into the North Atlantic Ocean—is very widely supported (Broecker, 1994, 2000; Broecker et al., 1992; Clement & Peterson, 2008; Sun et al., 2012).

Alley et al. (1999) have explained the role of thermohaline circulation in the formation of D-O oscillations and Heinrich events, and proposed three modes of North Atlantic Ocean conveyor belt (modern mode, glacial mode, Heinrich mode). During the Heinrich mode, the substantial freshwater flux into the North Atlantic Ocean constrains North Atlantic Deep Water (NADW) formation, which leads to the virtual collapse of AMOC. Across much of the Northern Hemisphere, climate appears to have responded to this in a matter of decades or less (e.g., Corrick et al., 2020; Denniston et al., 2007; Lea et al., 2003; Steffensen et al., 2008). Amplified by land-air-sea interactions (Clemens, 2005; Clement & Peterson, 2008), the influence of the collapse of AMOC on the climate over mid-latitude Asia is profound and the response to Heinrich events of spring and summer signals recorded in the loess record of the CLP and SCA is well detected.

During D-O oscillations, the variation of summer signals (precipitation in the CLP and dust activities in SCA) was much less, even undetectable, compared with the spring signals (precipitation in SCA and dust activities in the CLP). It has been suggested that the AMOC does not shut down completely in the glacial mode (Alley et al., 1999) and that NADW continues to be formed in parts of the North Atlantic Ocean. The impact of reduced AMOC on climate over mid-latitude Asia is much less marked than in the Heinrich mode, although it is still evident in the geological record. It has been suggested that the summer signals recorded in loess sections over mid-latitude Asia are not only affected by the weakened AMOC (Sun et al., 2012; Zhang & Delworth, 2005), but also modulated or overprinted by other processes originating from the tropical Pacific Ocean and Southern Ocean (Clement et al., 2001; Huang & Tian, 2008; Ivanochko et al., 2005; Lea, 2000; Rosenthal et al., 2003; Yin & Battisti, 2001). Spring signals on the other hand are more directly affected by North Atlantic Ocean and northern high-latitude atmospheric circulation (Aizen et al., 2001; Ding et al., 1995, 1998; Li & Wang, 2003; Yang & Ding, 2014) and, over mid-latitude Asia, are therefore more sensitive to abrupt climate events during the D-O oscillations of the last glacial.

6. Conclusions

In this study, we investigated the response of seasonal precipitation and dust activity over mid-latitude Asia to millennial-scale oscillations during the last glaciation. First, based on observations of modern processes, χ and Mz can be interpreted as representing summer precipitation and spring dust activity in the CLP, and as representing spring precipitation and summer activity in SCA. Second, by using EEMD and spectral analysis, seven IMFs were analyzed and the millennial-scale components presented similar periodicities to the Heinrich events and D-O oscillations recorded in the NGRIP $\delta^{18}O$. From the analyzed millennial-scale χ (Mz) components, it is evident that the DK section is more (less) sensitive to abrupt climate oscillations than sections in the CLP during the D-O oscillations. During Heinrich events, analyzed millennial-scale χ and Mz components exhibit distinct variations.

Given the observed distinct seasonal variations in precipitation and dust activity, it is proposed that the spring signals (precipitation in SCA and dust activity in the CLP) are more sensitive to abrupt climate events than the summer signals during the D-O oscillations, and that the seasonal signals are more highly variable

during Heinrich events. Our climatic proxies are verified by using simulations which reveal that signals during spring are more sensitive to meltwater forcing than summer signals in both the CLP and SCA. The weakening or complete shutdown of AMOC are thought to influence the response of seasonal signals to abrupt climate events. More high-resolution climate proxies with clear interpretation of seasonality are required to deepen our understanding of the response in geological deposits over mid-latitude Asia to the Northern Hemisphere high-latitude rapid climate events.

Data Availability Statement

The EEMD data for the loess sections will be accessible on figshare repository (from https://figshare.com/s/d5c182a650afa9c0fc32).

Acknowledgments
This work was supported by the National Natural Science Foundation of China (Grant No. 41771213 and 41877444) and the Second Tibetan Plateau Scientific Expedition and Research Program (Grant 2019QZKK0602). We thank anonymous reviewers for their critical reviews of the manuscript, and editor for his editorial support.

References

Ahn, J., & Brook, E. J. (2008). Atmospheric CO_2 and climate on millennial time scales during the last glacial period. *Science*, *322*, 83–85. https://doi.org/10.1126/science.1160832

Aizen, E. M., Aizen, V. B., Melack, J. M., Nakamura, T., & Ohta, T. (2001). Precipitation and atmospheric circulation patterns at mid-latitudes of Asia. *International Journal of Climatology*, *21*, 535–556. https://doi.org/10.1002/joc.626

Alley, R. B., Clark, P. U., Keigwin, L. D., & Webb, R. S. (1999). Making sense of millennial-scale climate change. *Geophysical Monograph Series*, *112*, 386–394. https://doi.org/10.1029/GM112p0385

Alley, R. B., Mayewski, P. A., Sowers, T., Stuiver, M., Taylor, K. C., & Clark, P. U. (1997). Holocene climatic instability: A prominent, widespread event 8200 yr ago. *Geology*, *25*, 483–486. https://doi.org/10.1130/0091-7613(1997)025<0483:hciapw>2.3.co;2

Altabet, M. A., Higginson, M. J., & Murray, D. W. (2002). The effect of millennial-scale changes in Arabian Sea denitrification on atmospheric CO_2. *Nature*, *415*, 159–162. https://doi.org/10.1038/415159a

An, Z. S., Kukla, G., Porter, S. C., & Xiao, J. L. (1991). Late Quaternary dust flow on the Chinese Loess Plateau. *Catena*, *18*, 125–132. https://doi.org/10.1016/0341-8162(91)90012-M

Balsam, W. L., Ellwood, B. B., Ji, J. F., Williams, E. R., Long, X. Y., & Hassani, A. E. (2011). Magnetic susceptibility as a proxy for rainfall: Worldwide data from tropical and temperate climate. *Quaternary Science Reviews*, *30*, 2732–2744. https://doi.org/10.1016/j.quascirev.2011.06.002

Barber, D. C., Dyke, A., Hillaire-Marcle, C., Jennings, A. E., Andrews, J. T., Kerwin, M. W., et al. (1999). Forcing of the cold event of 8,200 years ago by catastrophic drainage of Laurentide lakes. *Nature*, *400*, 344–348. https://doi.org/10.1038/22504

Blunier, T., & Brook, E. J. (2001). Timing of millennial-scale climate change in Antarctica and Greenland during the last glacial period. *Science*, *291*, 109–112. https://doi.org/10.1126/science.291.5501.109

Bond, G., Broecker, W., Johnsen, S., McManus, J., Labeyrie, L., Jouzel, J., & Bonani, G. (1993). Correlations between climate records from North Atlantic sediments and Greenland ice. *Nature*, *365*, 143–147. https://doi.org/10.1038/365143a0

Bova, S., Rosenthal, Y., Liu, Z. Y., Godad, S. P., & Yan, M. (2021). Seasonal origin of the thermal maxima at the Holocene and the last interglacial. *Nature*, *589*, 548–553. https://doi.org/10.1038/s41586-020-03155-x

Brewer, S., Guiot, J., & Torre, F. (2007). Mid-Holocene climate change in Europe: A data-model comparison. *Climate of the Past*, *3*, 499–512. https://doi.org/10.5194/cp-3-499-2007

Broecker, W. S. (1994). Massive iceberg discharges as a triggers for global climate change. *Nature*, *372*(6505), 421–424. https://doi.org/10.1038/372421a0

Broecker, W. S. (1998). Paleocean circulation during the last deglaciation: A bipolar seesaw? *Paleoceanography*, *13*, 119–121. https://doi.org/10.1029/97PA03707

Broecker, W. S. (2000). Was a change in thermohaline circulation responsible for the Little Ice Age? *Proceedings of the National Academy of Sciences*, *97*(4), 1339–1342. https://doi.org/10.1073/pnas.97.4.1339

Broecker, W. S., Bond, G., Klas, M., Clark, E., & McManus, J. (1992). Origin of the northern Atlantic's Heinrich events. *Climate Dynamics*, *6*, 265–273. https://doi.org/10.1007/BF00193540

Burns, S. J., Fleitmann, D., Matter, A., Kramers, J., & Al-Subbary, A. A. (2003). Indian Ocean climate and an absolute chronology over Dansgaard/Oeschger events 9 to 13. *Science*, *301*, 1365–1367. https://doi.org/10.1126/science.1086227

Cai, Y. J., Fung, I. Y., Edwards, R. L., An, Z. S., Cheng, H., Lee, J. E., et al. (2015). Variability of stalagmite-inferred Indian monsoon precipitation over the past 252,000 y. *Proceedings of the National Academy of Sciences*, *112*, 2954–2959. https://doi.org/10.1073/pnas.1424035112

Chen, F. H., Jia, J., Chen, J. H., Li, G. Q., Zhang, X. J., Xie, H. C., et al. (2016). A persistent Holocene wetting trend in arid central Asia, with wettest conditions in the late Holocene, revealed by multi-proxy analyses of loess-palolos sequences in Xinjiang, China. *Quaternary Science Reviews*, *146*, 134–146. https://doi.org/10.1016/j.quascirev.2016.06.002

Cheng, H., Edwards, R. L., Wang, Y. J., Kong, X. G., Ming, Y. F., Kelly, M. J., et al. (2006). A penultimate glacial monsoon record from Hulu Cave and two-phase glacial terminations. *Geology*, *34*, 217–220. https://doi.org/10.1130/G22289.1

Cheng, H., Zhang, H. W., Spötl, C., Baker, J., Sinha, A., Li, H. Y., et al. (2020). Timing and structure of the Younger Dryas event and its underlying climate dynamics. *Proceedings of the National Academy of Sciences*, *117*, 23408–23417. https://doi.org/10.1073/pnas.2007869117

Clemens, S. C. (2005). Millennial-band climate spectrum resolved and linked to centennial-scale solar cycles. *Quaternary Science Reviews*, *24*, 521–531. https://doi.org/10.1016/j.quascirev.2004.10.015

Clement, A. C., Cane, M. A., & Seager, R. (2001). An orbitally driven tropical source for abrupt climate change. *Journal of Climate*, *14*, 2369–2375. https://doi.org/10.1175/1520-0442(2001)014<2369:AODTSF>2.0.CO;2

Clement, A. C., & Peterson, L. C. (2008). Mechanisms of abrupt climate change of the last glacial period. *Reviews of Geophysics*, *46*, RG4002. https://doi.org/10.1029/2006RG000204

Corrick, E. C., Drysdale, R. N., Hellstromet, J. C., Capron, E., Rasmussen, S. O., Zhang, X., et al. (2020). Synchronous timing of abrupt climate changes during the last glacial period. *Science*, *369*, 963–969. https://doi.org/10.1126/science.aay5538

Dannenmann, S., Linsley, B. K., Oppo, D. W., Rosenthal, Y., & Beaufort, L. (2003). East Asian monsoon forcing of suborbital variability in the Sulu Sea during Marine Isotope Stage 3: Link to Northern Hemisphere climate. *Geochemistry, Geophysics, Geosystem*, *4*, 1–13. https://doi.org/10.1029/2002GC000390

Dansgaard, W., Johnsen, S. J., Clausen, H. B., Dahl-Jensen, D., Gundestrup, N. S., Hammer, C. U., et al. (1993). Evidence for general instability of past climate from a 250-kyr ice-core record. *Nature*, *364*, 218–220. https://doi.org/10.1038/364218a0

Deng, C. L., Liu, Q. S., Pan, Y. X., & Zhu, R. X. (2007). Environmental magnetism of Chinese loess-paleosol sequence. *Quaternary Sciences*, *27*, 193–209. (in Chinese with English abstract).

Denniston, R. F., Asmerom, Y., Polyak, V., Dorale, J. A., Carpenter, S. J., Trodick, C., et al. (2007). Synchronous millennial-scale climatic changes in the Great Basin and the North Atlantic during the last interglacial. *Geology*, *35*, 619–622. https://doi.org/10.1130/g23445a.1

Ding, Z. L., Liu, T. S., Rutter, N. W., Yu, Z. W., Guo, Z. T., & Zhu, R. X. (1995). Ice-volume forcing of East Asian winter monsoon variations in the past 800,000 years. *Quaternary Research*, *44*, 149–159. https://doi.org/10.1006/qres.1995.1059

Ding, Z. L., Ranov, V., Yang, S. L., Finaev, A., Han, J. M., & Wang, G. A. (2002). The loess record in southern Tajikistan and correlation with Chinese loess. *Earth and Planetary Science Letters*, *200*, 387–400. https://doi.org/10.1016/s0012-821x(02)00637-4

Ding, Z. L., Rutter, N. W., Liu, T. S., Sun, J. M., Ren, J. Z., Rokosh, D., & Xiong, S. F. (1998). Correlation of Dansgaard-Oeschger cycles between Greenland ice and Chinese loess. *Paleoclimates*, *2*, 281–291.

Ding, Z. L., Sun, J. M., Rutter, N. W., Rokosh, D., & Liu, T. S. (1999). Changes in the sand content of loess deposits along a north to south transect of the Chinese Loess Plateau and the implications for desert variations. *Quaternary Research*, *52*, 56–62. https://doi.org/10.1006/qres.1999.2045

Dodonov, A. E., Sadchikova, T. A., Sedov, S. N., Simakova, A. N., & Zhou, L. P. (2006). Multidisciplinary approach for paleoenvironmental reconstruction in loess-paleosol studies of the Darai Kalon section, southern Tajikistan. *Quaternary International*, *152*, 48–58. https://doi.org/10.1016/j.quaint.2005.12.001

Finaev, A. F. (2014). The model of dust aerosol accumulation in Tajikistan. *Geography Environment Sustainability*, *7*, 97–107. https://doi.org/10.24057/2071-9388-2014-7-3-97-107

Forster, T., & Heller, F. (1997). Magnetic enhancement paths in loess sediments from Tajikistan, China and Hungary. *Geophysical Research Letters*, *24*, 17–20. https://doi.org/10.1029/96gl03751

Gildor, H., & Tziperman, E. (2003). Sea-ice switches and abrupt climate change. *Philosophical Transactions of the Royal Society A: Mathematical, Physical & Engineering Sciences*, *361*, 1935–1944. https://doi.org/10.1098/rsta.2003.1244

Grootes, P. M., Stuiver, M., White, J. W. C., Johnsen, S., & Jouzel, J. (1993). Comparison of oxygen isotope records from the GISP2 and GRIP Greenland ice cores. *Nature*, *366*, 552–554. https://doi.org/10.1038/366552a0

Guo, F., Clemens, S. C., Wang, T., Wang, Y., Liu, Y. M., Liu, X. X., et al. (2020). Monsoon variations inferred from high-resolution geochemical records of the Linxia loess/paleosol sequence, western Chinese Loess Plateau. *Catena*, *198*, 105019. https://doi.org/10.1016/j.catena.2020.105019

Huang, E. Q., & Tian, J. (2008). Melt-Water-Pulse events and abrupt climate change of the last deglaciation. *Chinese Science Bulletin*, *53*, 1437–1447. (in Chinese with English abstract). https://doi.org/10.1007/s11434-008-0206-8

Huang, N. E., & Wu, Z. (2008). A review on Hilbert-Hung transform: Method and its applications to geophysical studies. *Reviews of Geophysics*, *46*, RG2006. https://doi.org/10.1029/2007rg000228

Huang, N. E., Zheng, S., Long, S. R., Wu, M. C., Shih, H. H., Zheng, Q., et al. (1998). The empirical mode decomposition and the Hilbert spectrum for nonlinear and non-stationary time series analysis. *Proceedings of the Royal Society of London*, *454*, 903–995. https://doi.org/10.2307/5316110.1098/rspa.1998.0193

Ivanochko, T. S., Ganeshram, R. S., Brummer, G. J. A., Ganssen, G., Jung, S. J. A., Moreton, S. G., & Kroon, D. (2005). Variations in tropical convection as an amplifier of global climate change at the millennial scale. *Earth and Planetary Science Letters*, *235*, 302–314. https://doi.org/10.1016/j.epsl.2005.04.002

Jia, J., Lu, H., Wang, Y. J., & Xia, D. S. (2018). Variations in the iron mineralogy of a loess section in Tajikistan during the mid-Pleistocene and late Pleistocene: Implications for the climatic evolution in Central Asia. *Geochemistry, Geophysics, Geosystems*, *19*, 1244–1258. https://doi.org/10.1002/2017GC007371

Jia, J., Zhu, L. D., Wang, Z. Y., Wang, B., & Chen, Q. (2019). The regional difference of climate evolution across mid-latitude Asia since mid-Pleistocene. *Quaternary Sciences*, *39*, 549–556. (in Chinese with English abstract).

Jiang, D. B., Lang, X. M., Tian, Z. P., & Wang, T. (2012). Considerable model-data mismatch in temperature over china during the mid-Holocene: Results of PMIP simulations. *Journal of Climate*, *25*, 4135–4153. https://doi.org/10.1175/jcli-d-11-00231.1

Jin, L. Y., Chen, F. H., Ganopolski, A., & Claussen, M. (2007). Response of East Asian climate to Dansgaard/Oeschger and Heinrich events in a coupled model of intermediate complexity. *Journal of Geophysical Research*, *112*, D06117. https://doi.org/10.1029/2006JD007316

Jin, L. Y., Chen, F. H., Morrill, C., Otto-Bliesner, B. L., & Rosenbloom, N. (2012). Causes of early Holocene desertification in arid central Asia. *Climate Dynamics*, *38*, 1577–1591. https://doi.org/10.1007/s00382-011-1086-1

Kalnay, E., Kanamitsu, M., Kistler, R., Collins, W., Deaven, D., Gandin, L., et al. (1996). The NCEP/NCAR 40-year reanalysis project. *Bulletin of the American Meteorological Society*, *77*, 437–471. https://doi.org/10.1175/1520-0477(1996)077<0437:tnyrp>2.0.co;2

Kang, S. G., Du, J. H., Wang, N., Dong, J. B., Wang, D., Wang, X. L., et al. (2020). Early Holocene weakening and mid- to late Holocene strengthening of the East Asian winter monsoon. *Geology*, *48*, 1043–1047. https://doi.org/10.1130/G47621.1

Karger, D. N., Conrad, O., Böhner, J., Kawohl, T., Kreft, H., Soria-Auza, R. W., et al. (2016). Climatologies at high resolution for the Earth land surface areas. *Scientific Data*, *4*, 170122. https://doi.org/10.1038/sdata.2017.122

Kleiven, H. F., Kissel, C., Laj, C., Ninnemann, U. S., Richter, T. O., & Cortijo, E. (2008). Reduced North Atlantic deep water coeval with the glacial Lake Agassiz freshwater outburst. *Science*, *319*(5859), 60–64. https://doi.org/10.1126/science.1148924

Knutti, R., Flückiger, J., Stocker, T. F., & Timmermann, A. (2004). Strong hemispheric coupling of glacial climate through freshwater discharge and ocean circulation. *Nature*, *430*, 851–856. https://doi.org/10.1038/nature02786

Lai, Z. P., & Wintle, A. G. (2006). Locating the boundary between the Pleistocene and the Holocene in Chinese loess using luminescence. *The Holocene*, *16*, 893–899. https://doi.org/10.1191/0959683606hol980rr

Lai, Z. P., Wintle, A. G., & Thomas, D. S. G. (2007). Rates of dust deposition between 50 ka and 20 ka revealed by OSL dating at Yuanbao on the Chinese Loess Plateau. *Palaeogeography, Palaeoclimatology, Palaeoecology*, *248*, 431–439. https://doi.org/10.1016/j.palaeo.2006.12.013

Lea, D. W., Pak, D. K., Peterson, L. C., & Hughen, K. A. (2003). Synchroneity of tropical and high-latitude Atlantic temperatures over the last glacial termination. *Science*, *301*, 1361–1364. https://doi.org/10.1126/science.1088470

Lea, D. W., Pak, D. K., & Spero, H. J. (2000). Climate impact of Late Quaternary Equatorial Pacific Sea surface temperature variations. *Science*, *289*, 1719–1724. https://doi.org/10.1126/science.289.5485.1719

Li, J. P., & Wang, J. X. L. (2003). A modified zonal index and its physical sense. *Geophysical Research Letters*, *30*, 1632. https://doi.org/10.1029/2003gl017441
Li, Y., Song, Y. G., Fitzsimmons, K. E., Chang, H., Orozbaev, R., & Li, X. X. (2018). Eolian dust dispersal patterns since the last glacial period in eastern Central Asia: Insights from a loess-paleosol sequence in the Ili Basin. *Climate of the Past*, *14*, 271–286. https://doi.org/10.5194/cp-14-271-2018
Li, Y., Song, Y. G., Kaskaoutis, D. G., Chen, X. L., Mamadjanov, Y., & Tan, L. C. (2019). Atmospheric dust dynamics in southern Central Asia: Implications for buildup of Tajikistan loess sediments. *Atmospheric Research*, *229*, 74–85. https://doi.org/10.1016/j.atmosres.2019.06.013
Li, Y., Song, Y. G., Lai, Z. P., Han, L., & An, Z. S. (2016). Rapid and cyclic dust accumulation during MIS2 in Central Asia inferred from loess OSL dating and grain size analysis. *Scientific Reports*, *6*, 32365. https://doi.org/10.1038/srep32365
Li, Y., Song, Y. G., Orozbaev, R., Dong, J. B., Li, X. Z., & Zhou, J. (2020). Moisture evolution in Central Asia since 26 ka: Insights from a Kyrgyz loess section, Western Tian Shan. *Quaternary Science Reviews*, *249*, 106604. https://doi.org/10.1016/j.quascirev.2020.106604
Li, Y., Song, Y. G., Yin, Q. Z., Han, L., & Wang, Y. X. (2019). Orbital and millennial northern mid-latitude westerlies over the last glacial period. *Climate Dynamics*, *53*, 3315–3324. https://doi.org/10.1007/s00382-019-04704-5
Li, Y., Su, N., Liang, L., Ma, L., Yan, Y., & Sun, Y. (2015). Multiscale monsoon variability during the last two climatic cycles revealed by spectral signals in Chinese loess and speleothem records. *Climate of the Past*, *11*, 1067–1075. https://doi.org/10.5194/cp-11-1067-2015
Liu, T. S. (1985). *Loess and the environment*. China Ocean Press.
Liu, Y., Liu, H., Song, H., Li, Q., Burr, G. S., Wang, L., & Hu, S. (2017). A monsoon-related 174-year relative humidity record from tree-ring $\delta^{18}O$ in the Yaoshan region, eastern central China. *Science of the Total Environment*, *593*, 523–534. https://doi.org/10.1016/j.scitotenv.2017.03.198
Liu, Z., Otto-Bliesner, B., He, F., Brady, E., Tomas, R., Clark, P., et al. (2009). Transient simulation of deglacial climate evolution with a new mechanism for Bølling-Allerød warming. *Science*, *325*, 310–314. https://doi.org/10.1126/science.1171041
Liu, Z. Y., Wen, X. Y., Brady, E. C., Otto-Bliesner, B., Yu, G., Lu, H. Y., et al. (2014). Chinese cave records and the East Asia Summer Monsoon. *Quaternary Science Reviews*, *83*, 115–128. https://doi.org/10.1016/j.quascirev.2013.10.021
Liu, Z. Y., Zhu, J., Rosenthal, Y., Zhang, X., Otto-Bliesner, B. L., Timmermann, A., et al. (2014). The Holocene temperature conundrum. *Proceedings of the National Academy of Sciences*, *111*, 3501–E3505. https://doi.org/10.1073/pnas.1407229111
Lohmann, G., Pfeiffer, M., Laepple, T., Leduc, G., & Kim, J. H. (2013). A model-data comparison of the Holocene global surface temperature evolution. *Climate of the Past*, *9*, 1807–1839. https://doi.org/10.1016/j.quaint.2012.08.1170
Lu, F. Z., Ma, C. M., Zhu, C., Lu, H. Y., Zhang, X. J., Huang, K. Y., et al. (2018). Variability of East Asian summer monsoon precipitation during the Holocene and possible forcing mechanisms. *Climate Dynamics*, *52*, 969–989. https://doi.org/10.1007/s00382-018-4175-6
Lu, H., Jia, J., Yin, Q. Z., Xia, D. S., Gao, F. Y., Liu, H., et al. (2020). Atmospheric dynamics patterns in southern Central Asia since 800 ka revealed by Loess-Paleosol sequences in Tajikistan. *Geophysical Research Letters*, *47*, e2020GL088320. https://doi.org/10.1029/2020GL088320
Lu, H. Y., Yang, Y. S., Xu, Z. W., Zhou, Y. L., Zeng, L., Zhu, F. Y., et al. (2013). Chinese deserts and sand fields in Last Glacial Maximum and Holocene Optimum. *Chinese Science Bulletin*, *58*, 2775–2783. https://doi.org/10.1007/s11434-013-5919-7
Maher, B. A. (1998). Magnetic properties of modern soils and Quaternary loessic paleosols: Paleoclimatic implications. *Palaeogeography, Palaeoclimatology, Palaeoecology*, *137*, 25–54. https://doi.org/10.1016/S0031-0182(97)00103-X
Meng, X. M., Derbyshire, E., & Kemp, R. A. (1997). Origin of the magnetic susceptibility signal in Chinese loess. *Quaternary Science Reviews*, *16*, 833–839. https://doi.org/10.1016/s0277-3791(97)00053-x
Ning, H. W., Wang, S. G., & Du, J. W. (2005). Characteristics of sand dust events and their influence on air quality of Xian city. *Journal of Desert Research*, *25*, 886–890. (in Chinese with English abstract).
North Greenland Ice Core Project Members. (2004). High-resolution record of Northern Hemisphere climate extending into the last interglacial period. *Nature*, *431*, 147–151. https://doi.org/10.1038/nature02805
Porter, S. C. (2001). Chinese loess record of monsoon climate during the last glacial interglacial cycle. *Earth-Science Reviews*, *54*, 115–128. https://doi.org/10.1016/s0012-8252(01)00043-5
Porter, S. C., & An, Z. S. (1995). Correlation between climate events in the North Atlantic and China during the last glaciation. *Nature*, *375*, 305–308. https://doi.org/10.1038/375305a0
Qiu, F. Y., & Zhou, L. P. (2015). A new luminescence chronology for the Mangshan loess-paleosol sequence on the southern bank of the Yellow River in Henan, central China. *Quaternary Geochronology*, *30*, 24–33. https://doi.org/10.1016/j.quageo.2015.06.014
Rao, Z. G., Chen, F. H., Cheng, H., Liu, W. G., Wang, G. A., Lai, Z. P., & Bloemendal, J. (2013). High-resolution summer precipitation variations in the western Chinese loess plateau during the last glacial. *Scientific Reports*, *3*, 2785. https://doi.org/10.1038/srep02785
Rosenthal, Y., Oppo, D. W., & Linsley, B. K. (2003). The amplitude and phasing of climate change during the last deglaciation in the Sulu Sea, western equatorial Pacific. *Geophysical Research Letters*, *30*, 1428. https://doi.org/10.1029/2002GL016612
Schiemann, R., Lüthi, D., Vidale, P. L., & Schär, C. (2008). The precipitation climate of Central Asia-intercomparison of observational and numerical data sources in a remote semiarid region. *International Journal of Climatology*, *28*, 295–314. https://doi.org/10.1002/joc.1532
Schneider, B., Leduc, G., & Park, W. (2010). Disentangling seasonal signals in Holocene climate trends by satellite-model-proxy integration. *Paleoceanography*, *25*. https://doi.org/10.1029/2009PA001893
Schulz, M., & Mudelsee, M. (2002). REDFIT: Estimating red-noise spectra directly from unevenly spaced paleoclimatic time series. *Computer Geosciences*, *28*, 421–426. https://doi.org/10.1016/S0098-3004(01)00044-9
Song, Y. G., Zeng, M. X., Chen, X. L., Li, Y., Chang, H., An, Z. S., & Guo, X. H. (2018). Abrupt climatic events recorded by the Ili loess during last glaciation in Central Asia: Evidence from grain-size and minerals. *Journal of Asian Earth Sciences*, *155*, 58–67. https://doi.org/10.1016/j.jseaes.2017.10.040
Steffensen, J. P., Andersen, K. K., Bigler, M., Clausen, H. B., Dahl-Jensen, D., Fischer, H., et al. (2008). High-resolution Greenland ice core data show abrupt climate change happens in few years. *Science*, *321*, 680–684. https://doi.org/10.1126/science.1157707
Sun, J. M. (2020). Loess deposits and its relationship with earth sphere interactions. *Quaternary Sciences*, *40*(1), 1–7. (in Chinese with English abstract).
Sun, J. M., Zhang, M. Y., & Liu, T. S. (2001). Spatial and temporal characteristics of dust storms in China and its surrounding regions, 1960–1999: Relations to source area and climate. *Journal of Geophysical Research*, *106*, 10325–10333. https://doi.org/10.1029/2000JD900665
Sun, Y. B., Clemens, S., Guo, F., Liu, X. X., Wang, Y., Yan, Y., & Liang, L. J. (2021). High-sedimentation-rate loess records: A new window into understanding orbital- and millennial-scale variability. *Earth-Science Reviews*, *220*, 103731. https://doi.org/10.1016/j.earscirev.2021.103731
Sun, Y. B., Clemens, S. C., Morrill, C., Lin, X. P., Wang, X. L., & An, Z. S. (2012). Influence of Atlantic meridional overturning circulation on the East Asian winter monsoon. *Nature Geoscience*, *5*, 46–49. https://doi.org/10.1038/ngeo1326

Sun, Y. B., & Guo, F. (2017). Rapid monsoon changes recorded by Chinese loess deposits. *Quaternary Sciences*, *37*, 963–973. (in Chinese with English abstract).
Sun, Y. B., Kutzbach, J., An, Z. S., Clemens, S., Liu, Z. Y., Liu, W. G., et al. (2015). Astronomical and glacial forcing of the East Asian summer monsoon variability. *Quaternary Science Reviews*, *115*, 132–142. https://doi.org/10.1016/j.quascirev.2015.03.009
Sun, Y. B., Liang, L. J., Bloemendal, J., Li, Y., Wu, F., Yao, Z. Q., & Liu, Y. G. (2016). High-resolution scanning XRF investigation of Chinese loess and its implications for millennial-scale monsoon variability. *Journal of Quaternary Science*, *31*, 191–202. https://doi.org/10.1002/jqs.2856
Sun, Y. B., Wang, X. L., Liu, Q. S., & Clemens, S. C. (2010). Impacts of post-depositional processes on rapid monsoon signals recorded by the last glacial loess deposits of northern China. *Earth and Planetary Science Letters*, *289*, 171–179. https://doi.org/10.1016/j.epsl.2009.10.038
Sundqvist, H. S., Zhang, Q., Moberg, A., Holmgren, K., Körnich, H., Nilsson, J., & Brattström, G. (2010). Climate change between the mid and late Holocene in northern high latitudes—Part 1: Survey of temperature and precipitation proxy data. *Climate of the Past*, *6*, 739–608. https://doi.org/10.5194/cp-6-591-2010
Tan, L. C., Li, Y. Z., Wang, X. Q., Cai, Y. J., Lin, F. Y., Cheng, H., et al. (2020). Holocene monsoon change and abrupt events on the western Chinese Loess Plateau as revealed by accurately-dated stalagmites. *Geophysical Research Letters*, *47*, e2020GL090273. https://doi.org/10.1029/2020GL090273
Torrent, J., Barron, V., & Liu, Q. S. (2006). Magnetic enhancement is linked to and precedes hematite formation in aerobic soil. *Geophysical Research Letters*, *33*, L02401. https://doi.org/10.1029/2005GL024818
Vandenberghe, J., Renssen, H., Huissteden, K., Nugteren, G., Konert, M., Lu, H. Y., et al. (2006). Penetration of Atlantic westerly winds into Central and East Asia. *Quaternary Science Reviews*, *25*, 2380–2389. https://doi.org/10.1016/j.quascirev.2006.02.017
Wang, P. X. (2009). Global monsoon in a geological perspective. *Chinese Science Bulletin*, *54*, 1113–1136. https://doi.org/10.1007/s11434-009-0169-4
Wang, Y., Guo, F., Man, L., Yan, Y., Liu, X. X., & Sun, Y. B. (2020). Millennial-scale summer monsoon oscillations over the last 260 ka revealed by high-resolution elemental results of the Mangshan loess-palaeosol sequence from the southeastern Chinese Loess Plateau. *Quaternary International*, *552*, 164–174. https://doi.org/10.1016/j.quaint.2020.05.039
Wang, Y. J., Cheng, H., Edwards, L. R., Kong, X. G., Shao, X. H., Chen, S. T., et al. (2008). Millennial-and orbital-scale changes in the East Asian monsoon over the past 224,000 years. *Nature*, *451*, 1090–1093. https://doi.org/10.1038/nature06692
Wang, Y. J., Jia, J., Liu, H., Lu, C. C., Xia, D. S., & Lu, H. (2018). The magnetic susceptibility recorded millennial-scale variability in central Asia during last glacial and interglacial. *Geophysical Journal International*, *215*, 1781–1788. https://doi.org/10.1093/gji/ggy378
Wu, L., Li, C., Yang, C., & Xie, S. P. (2008). Global teleconnections in response to a shutdown of the Atlantic meridional overturning circulation. *Journal of Climate*, *21*, 3002–3019. https://doi.org/10.1175/2007JCL1858.1
Wu, Z., & Huang, N. E. (2009). Ensemble empirical mode decomposition: A noise-assisted data analysis method. *Advances in Adaptive Data Analysis*, *1*, 1–41. https://doi.org/10.1142/S1793536909000047
Xiao, J. L., Porter, S. C., An, Z. S., Kumai, H., & Yoshikawa, S. (1995). Grain size of quartz as an indicator of winter monsoon strength on the Loess Plateau of central China during the last 130,000 yr. *Quaternary Research*, *43*, 22–29. https://doi.org/10.1006/qres.1995.1003
Yang, L. W., & Jia, J. (2021). Temperature dependence of pedogenic magnetic mineral formation in loess deposits. *Quaternary International*, *580*, 95–99. https://doi.org/10.1016/j.quaint.2021.01.022
Yang, S. L., Ding, F., & Ding, Z. L. (2006). Pleistocene chemical weathering history of Asian arid and semi-arid regions recorded in loess deposits of China and Tajikistan. *Geochimica et Cosmochimica Acta*, *70*, 1695–1709. https://doi.org/10.1016/j.gca.2005.12.012
Yang, S. L., & Ding, Z. L. (2006). Winter-spring precipitation as the principal control on predominance of C_3 plants in the Central Asia over the past 1.77 Myr: Evidence from $\delta^{13}C$ of loess organic matter in Tajikistan. *Palaeogeography, Palaeoclimatology, Palaeoecology*, *225*, 330–339. https://doi.org/10.1016/j.palaeo.2005.11.007
Yang, S. L., & Ding, Z. L. (2008). Advance-retreat history of the East-Asian summer monsoon rainfall belt over northern China during the last two glacial-interglacial cycles. *Earth and Planetary Science Letters*, *274*, 499–510. https://doi.org/10.1016/j.epsl.2008.08.001
Yang, S. L., & Ding, Z. L. (2014). A 249 kyr stack of eight loess grain size records from northern China documenting millennial-scale climate variability. *Geochemistry, Geophysics, Geosystems*, *15*, 798–814. https://doi.org/10.1002/2013GC005113
Yin, J. H., & Battisti, D. S. (2001). The importance of tropical sea surface temperature patterns in simulations of Last Glacial Maximum climate. *Journal of Climate*, *14*, 565–581. https://doi.org/10.1175/1520-0442(2001)014<0565:tiotss>2.0.co;2
Yu, G., Chen, X., Liu, J., & Wang, S. M. (2000). Simulation and diagnosis of east Asian climate during the Last Glacial Maximum. *Science Bulletin*, *20*, 2153–2159. (in Chinese with English abstract).
Zhang, R., & Delworth, T. L. (2005). Simulated tropical response to a substantial weakening of the Atlantic thermohaline circulation. *Journal of Climate*, *18*, 1853–1860. https://doi.org/10.1175/JCLI3460.1
Zhang, W. X., Shi, Z. T., Liu, Y., Su, H., & Niu, J. (2015). Climate record in the loess-paleosol sediment in the Ili basin of Xinjiang and comparative analysis with the Heinrich events. *Journal of Glaciology and Geocryology*, *37*(4), 973–979. (in Chinese with English abstract).
Zhao, M., Huang, C. Y., Wang, C. C., & Wei, G. (2006). A millennial-scale UK^{37} sea-surface temperature record from the South China Sea (8°C) over the last 150 kyr: Monsoon and sea-level influence. *Palaeogeography, Palaeoclimatology, Palaeoecology*, *236*, 39–55. https://doi.org/10.1016/j.palaeo.2005.11.033